

Analytical Methods

Accepted Manuscript



This is an *Accepted Manuscript*, which has been through the Royal Society of Chemistry peer review process and has been accepted for publication.

Accepted Manuscripts are published online shortly after acceptance, before technical editing, formatting and proof reading. Using this free service, authors can make their results available to the community, in citable form, before we publish the edited article. We will replace this *Accepted Manuscript* with the edited and formatted *Advance Article* as soon as it is available.

You can find more information about *Accepted Manuscripts* in the [Information for Authors](#).

Please note that technical editing may introduce minor changes to the text and/or graphics, which may alter content. The journal's standard [Terms & Conditions](#) and the [Ethical guidelines](#) still apply. In no event shall the Royal Society of Chemistry be held responsible for any errors or omissions in this *Accepted Manuscript* or any consequences arising from the use of any information it contains.

1
2
3
4 1 Silica-Based Surface Molecularly Imprinting for Recognition and
5
6 2 Separation of Lysozyme
7
8
9 3

10 4 Cenjin Zhang^a, Yuzhi Wang^{a*}, Yigang Zhou^{b*}, Junxia Guo^a, Yanjin Liu^a
11 5
12 6
13 7

14 8
15 9 ^a State Key Laboratory of Chemo/Biosensing and Chemometrics, College of
16 10 Chemistry and Chemical Engineering, Hunan University, Changsha, 410082, P.R.
17 11 China
18 12
19 13

20 14 ^b Department of Microbiology, College of Basic Medicine, Central South
21 15 University, Changsha, 410083, P.R. China
22 16
23 17
24 18
25 19
26 20
27 21
28 22
29 23
30 24

31 25 **Corresponding author: Professor Yuzhi Wang; Associate professor Yigang Zhou**
32 26
33 27
34 28

35 29 State Key Laboratory of Chemo/Biosensing and Chemometrics
36 30
37 31
38 32
39 33
40 34
41 35
42 36
43 37
44 38
45 39
46 40
47 41
48 42
49 43
50 44
51 45
52 46
53 47
54 48
55 49
56 50
57 51
58 52
59 53
60 54

55 55 College of Chemistry and Chemical Engineering
56 56
57 57
58 58
59 59
60 60

61 61 Hunan University
62 62
63 63
64 64
65 65
66 66
67 67
68 68
69 69
70 70

71 71 Changsha 410082
72 72
73 73
74 74
75 75
76 76
77 77
78 78
79 79
80 80

81 81 P. R. China
82 82
83 83
84 84
85 85
86 86
87 87
88 88
89 89
90 90

91 91 Phone: +86-731-88821903
92 92
93 93
94 94
95 95
96 96
97 97
98 98
99 99
100 100

101 101 Fax: +86-731-88821848
102 102
103 103
104 104
105 105
106 106
107 107
108 108
109 109
110 110

111 111 E-mail: wyzss@hnu.edu.cn
112 112
113 113
114 114
115 115
116 116
117 117
118 118
119 119
120 120

121 121 **Abbreviations:** APTES, 3-aminopropyltriethoxysilane; BSA, bovine serum albumin; BHB,
122 122
123 123
124 124
125 125
126 126
127 127
128 128
129 129
130 130

131 131 bovine hemoglobin; FT-IR, fourier transform infrared spectroscopy; Lyz, lysozyme; MIP,
132 132
133 133
134 134
135 135
136 136
137 137
138 138
139 139
140 140

1
2
3
4 25 molecularly imprinted polymer; NIP, non-imprinted polymer; OVA, ovalbumin; PB, phosphate
5
6 26 buffer solution; SDS, sodium dodecyl sulfate; TEM, transmission electron microscope; TEOS,
7
8
9 27 tetraethoxysilane; TG, thermogravimetric analysis;

10
11 28

12
13
14 29 **Key Words:** Surface molecular imprinting / Silica-based / Sol-gel /Lysozyme/ Recognition

15
16 30

17
18 31

19
20 32

21
22 33

23
24 34

25
26 35

27
28 36

29
30 37

31
32 38

33
34 39

35
36 40

37
38 41

39
40 42

41
42 43

43
44 44

45
46 45

47
48 46

47 **Abstract**

48 A highly selective surface molecular imprinting inorganic polymer composed of
49 tetraethoxysilane and 3-aminopropyltriethoxysilane has been prepared by a sol–gel process on silica
50 submicroparticles in aqueous solution under simple and mild conditions. Lysozyme (Lyz, pI 11,
51 MW 14.4 kDa) is used as the template protein. Product polymers were characterized by FT-IR, TEM,
52 and TG techniques to verify the successful synthesis of the MIP on the surface of silica
53 submicroparticles. The adsorption behavior of MIP was evaluated by adsorption capacity, imprint
54 factor and adsorption model. It was found that both MIP and NIP could adsorb template protein
55 quickly and easily owing to the low mass transfer resistance of thin shell and their adsorption
56 equilibrium could be reached in 5h. Compared with NIP, MIP showed stronger adsorption capacity
57 for template protein Lyz under all experimental conditions. The mechanism for static adsorption of
58 Lyz onto MIP was found to follow Langmuir adsorption model which was further used to calculate
59 the maximum adsorption capacity Q_{\max} and gave a result of 90.33 mg/g in theory. The MIP
60 adsorbent could be reuse twice without significant loss in adsorption capacity. MIP indicated
61 excellent recognition and binding affinity toward Lyz, whose selectivity factor β for Lyz relative to
62 reference proteins bovine serum albumin (BSA, pI 4.9, MW 69.0 kDa), bovine hemoglobin (BHb, pI
63 6.9, MW 65.0kDa) and ovalbumin (OVA, pI 4.7, MW 43.0kDa) were 2.36, 2.22, and 2.24,
64 respectively. It was shown that the shape memory and the size effect were the major factors for the
65 recognition. This imprinted inorganic polymer was used to specifically adsorb the Lyz from the
66 protein mixture, which demonstrated its potential selectivity.

69 Introduction

70
71 Molecular imprinting is a technique for preparing recognition sites with predetermined
72 selectivity which are tailor-made in situ by copolymerization of functional monomers and cross
73 linkers in the presence of template molecule^[1-2]. After removal of the template molecule from the
74 polymer network, specific recognition sites that are complementary to the template in terms of
75 their size, shape, and functionality are exposed^[3]. Because of its excellent advantages like specific
76 recognition, high stability, low cost and its reusability, MIP material has been successfully applied
77 to the fields of biosensors^[4-5], solid-phase extraction^[6-8], separation^[9-10], catalysis^[11-12], and drug
78 delivery^[13] over the past decades. Despite the attractive features of MIP material with specificity, it
79 has been largely limited to small molecules. The imprinting of biological macromolecules and
80 proteins still remains to be a challenge due to their incompatibility of these targets with organic
81 solvents that are typically used for imprinting.

82 Protein molecularly imprinted technique is a method for separation which use the protein as
83 template to prepare the molecularly imprinted polymers (MIP). The MIP has a spatial structure
84 complementary with template, so it can specifically recognize the target protein. Because protein
85 has characteristics of large molecular size, the high flexibility of conformation, the complex
86 surface structures, there are still many challenges to imprint protein^[14]. Therefore, it is necessary
87 to study deeply about the preparation of protein imprinted polymers. The protein imprinted
88 polymers can be used as cell scaffold material, antibodies and enzymes, which can substitute for
89 natural biological structure^[15-17]. For the above reason the protein MIPs have a widely application
90 in biomedical field.

91 However, due to the thick polymeric network, the MIPs prepared by the conventional bulky

1
2
3
4 92 polymerization technique had some disadvantages especially for protein imprinting, such as poor
5
6 93 site accessibility to the target molecules and low rebinding capacity ^[18-19]. The protein template
7
8
9 94 molecules were entrapped deeply in the matrices, the elution was difficult, the diffusion barrier for
10
11 95 the template molecules was higher, the rate of mass transfer was lower, and the template
12
13 96 molecules were not easy to bind with recognition sites ^[20-21]. These drawbacks can be effectively
14
15
16 97 avoided by surface molecular imprinting approach, which provides an alternative way for
17
18
19 98 improving mass transfer, increasing affinity binding and decreasing high diffusion barrier of the
20
21 99 template by fixing MIP on a support substrate ^[22]. For surface molecular printing, TiO₂ ^[23], Fe₂O₃
22
23
24 100 ^[24], and carbonaceous materials ^[25] had already been used as solid support materials. However,
25
26
27 101 SiO₂ was the most commonly used solid support materials reported by numerous studies ^[26-30].

28
29 102 In this work, a highly selective surface molecular imprinting polymer for Lyz was
30
31 103 synthesized on the support of silica submicroparticles by a sol-gel process which could create the
32
33
34 104 uniform and small sizes of the particles and offer high surface area for the regeneration of template.
35
36 105 APTES and TEOS were chosen as functional monomer and cross linker, respectively. The MIP
37
38
39 106 was characterized by FT-IR, TEM, TG techniques. Imprinting efficiency of MIP was investigated
40
41 107 by static adsorption tests. The resulting imprinted polymer (MIP) showed better template affinity
42
43
44 108 than the corresponding non-imprinted polymer (NIP). The selectivity of the obtained polymer was
45
46
47 109 evaluated over competitive compounds, and the results demonstrated that the MIP was capable of
48
49
50 110 selective recognition of Lyz.

51
52 111 Compared with the conventional method, most of the recognition sites generated for surface
53
54 112 imprinting would be on the thin outer shell layer, with a greatly increased accessibility and
55
56
57 113 effectiveness. Moreover submicron structured MIPs have a small dimension with extremely high
58
59
60

1
2
3
4 114 surface-to-volume ratio, so that most of template molecules are situated at the surface or in the
5
6 115 proximity of the material's surface. Obviously, submicro-sized surface imprinting MIPs are
7
8
9 116 expected to improve the binding capacity, binding kinetics and accessibility of the recognition
10
11 117 sites, especially for protein molecular imprinting in which the mass transfer limitation may be a
12
13
14 118 more pronounced problem.

15
16 119 This surface molecular imprinting polymer was shown to be promising for regeneration and
17
18
19 120 can be potentially employed as a generally applicable methodology for protein imprinting.
20

21 121

22 122 **Experimental sections**

23 123 **Instrumentation**

24
25
26 124 A UV-2450 UV-vis spectrophotometer (Shimadzu, Japan) was used to determine the
27
28
29 125 absorbance of protein. FTIR spectra were recorded on a Spectrum One FTIR spectrometer (Perkin
30
31
32 126 Elmer, U.S.). Thermal gravimetry (TG) curves of samples were acquired by STA409 thermal
33
34
35 127 gravimetric analyzer (Netzsch, Germany). Virtis freeze drier (YiKang Experimental Equipment
36
37
38 128 Co. Ltd, Beijing, China) was employed to get the freeze-dried polymers. After being dried, the
39
40
41 129 samples were imaged under a JEOL JEM-3010 transmission electron microscopy.
42
43
44 130

45 131 **Chemicals and reagents**

46
47
48 132 3-aminopropyltriethoxysilane (APTES) was supplied by Aladdin chemistry Co., Ltd.
49
50
51 133 (Shanghai, China). Tetraethoxysilane (TEOS) was bought from Shanghai Titan chemistry Co., Ltd.
52
53
54 134 (Shanghai, China). Acetic acid, anhydrous ethanol, ammonium hydroxide, lysozyme (Lyz, pI 11,
55
56
57 135 MW 14.4 kDa), bovine serum albumin (BSA, MW 69kDa, pI 4.9), bovine hemoglobin (BHb, MW
58
59
60

1
2
3
4 136 65kDa, pI 6.9), ovalbumin (OVA, pI 4.7, MW 43.0kDa) were all purchased from Guoyao
5
6 137 chemical reagents company Co., Ltd. (China). Phosphate buffer solution (pH 7.0, 10 mM) was
7
8 138 used as the working medium. All chemicals used were of analytical grade and used directly
9
10 139 without further purification. Ultrapure water ($18.25\text{M}\Omega\text{ cm}^{-1}$) used throughout the experiment was
11
12 140 obtained from the laboratory purification system.
13
14
15
16
17
18

19 142 **Preparation of Silica Submicroparticles**

20
21 143 Silica submicroparticles were synthesized by the hydrolysis of TEOS with ammonium
22
23 144 hydroxide following a procedure described by Stöber et al ^[31]. In this experiment, 4.5 mL of TEOS
24
25 145 was resolved in a mixture containing total 48.9 mL of aqueous ammonia (25% concentrated
26
27 146 ammonia in water), 9 mL of H₂O and 37.6 mL of anhydrous ethanol. The system was stirred at
28
29 147 room temperature for 5 h, resulting in the formation of white silica colloidal suspension. The silica
30
31 148 submicroparticles were centrifugally separated from the suspension and washed with anhydrous
32
33 149 ethanol several times until eluent became neutral. Finally, the SiO₂ submicroparticles were dried
34
35 150 under vacuum overnight.
36
37
38
39
40
41
42

43 152 **Preparation of Imprinted and Non-imprinted Polymers**

44
45 153 The surface molecular imprinting inorganic polymers were synthesized by a sol-gel process
46
47 154 on silica submicroparticles polymerized with APTES and TEOS in aqueous solution. At first, 400
48
49 155 mg silica submicroparticles were dispersed in mixture solution containing 20 mL of ethanol and
50
51 156 20 mL of phosphate buffer solution (pH 7.0, 10 mM) by ultrasonic vibration for 10 minutes. Then,
52
53 157 0.1 g of template protein Lyz and 0.62 mL of APTES were added into the suspension under
54
55
56
57
58
59
60

1
2
3
4 158 stirring for 2 h to obtain the completely self-assembled composites on silica submicroparticles.
5
6 159 Finally, 1.24 mL of TEOS and 1 mL of HAc (1.0 mol L⁻¹) were added to the mixture suspension
7
8
9 160 at room temperature under stirring for 18h to obtain particles with a high cross-linking structure.
10
11 161 After reaction the obtained polymer was first washed with SDS-HAc (10%w/v: 10%v/v) to
12
13 162 remove the template molecules for several times until no Lyz could be detected by a UV-vis
14
15 163 spectrophotometer at 278 nm and then washed with ultrapure water to remove SDS. The product
16
17 164 polymer was dried at 60 °C for 12 h under vacuum. The non-imprinted polymer (NIP) was
18
19 165 prepared and treated by the same conditions without the addition of template protein Lyz. The
20
21 166 synthesis of MIP was shown in Fig 1. For comparison, several polymers with different
22
23 167 cross-linking degrees were prepared by adjusting the reactant ratio of the volume of TEOS and
24
25 168 APTES which were summarized in table 1.
26
27
28
29
30
31
32
33

34 170 **Characterization of polymers**

35
36 171 The MIP and NIP were characterized by FT-IR spectra and TEM. FT-IR spectra (4000–400
37
38 172 cm⁻¹) in KBr were recorded using a Spectrum One FTIR spectrometer (Perkin Elmer, U.S.). The
39
40 173 morphologies of the polymers were determined by a JEOL JEM-3010 transmission electron
41
42 174 microscopy. The polymers were coated with a thin layer of gold under vacuum and photographed
43
44 175 by the TEM. The average particle sizes of the particles were determined on the TEM images
45
46 176 based on a weighted-averages method. Thermal gravimetry (TG) curves of polymers were
47
48 177 acquired by using a thermoanalysis instrument under dynamic nitrogen atmosphere at a heating
49
50 178 rate of 10 °C min⁻¹.
51
52
53
54

55 179 **Determination of Equilibrium Swelling Ratio**

1
2
3
4 180 The freeze-dried silica-based polymers and silica submicroparticles were prepared by virtis freeze
5
6 181 drier after frozen totally in refrigerator. The freeze-dried polymers with specific weight were immersed
7
8 182 in phosphate buffer solution (pH 7.0, 10 mM) at room temperature overnight. After equilibrium, the
9
10 183 polymers were taken out and isolated by centrifugation at 12 000 rpm for 30 min. Measurement of the
11
12 184 polymers swollen weight (M_s) was made after the supernatant was removed. Subsequently, the
13
14 185 polymers were dried at room temperature in vacuum box and weighed again to obtain the dry weight
15
16 186 (M_d). The Swelling Ratio (SR) was defined by the following formula:

17
18
19
20
21
22 187
$$SR = \frac{M_s - M_d}{M_d} \quad (1)$$

23
24

25 188 Where M_d and M_s Represent the weight of the dry and swollen samples respectively.
26
27
28 189

30 190 **Static adsorption experiments**

31
32 191 The freeze-dried imprinted and non-imprinted polymers (10.0 mg) were incubated in 5.0 mL of a
33
34 192 series of different concentrations of Lyz solution for 24 hours. All the binding experiments were
35
36 193 conducted by the incubator shaker (200 r/min, 25°C). After adsorption equilibrium, samples were
37
38 194 centrifuged with a centrifuge at 8000 rpm for 8 min. The concentration of Lyz in the supernatant
39
40 195 was detected by an UV-2450 UV-vis spectrophotometer (Shimadzu, Japan) at the
41
42 196 wavelength of 278 nm used phosphate buffer solution (pH 7.0, 10 mM) as solvent under
43
44 197 room temperature.
45
46
47
48

49
50 198 The amount of adsorbed protein was evaluated from the following formula:

51
52 199
$$Q = \frac{(C_0 - C)V}{M} \quad (2)$$

53
54

55 200 Where Q is the mass of protein adsorbed onto a unit amount of dry polymer (mg /g), C_0 and C are the
56
57 201 initial and equilibrium concentrations of protein solutions respectively (mg /mL), V is the initial
58
59
60

202 volume of the solutions (mL), and M is the mass of dry polymer (g).

203 The imprinting factor α was defined by following formula:

$$204 \quad \alpha = Q_{\text{MIP}}/Q_{\text{NIP}} \quad (3)$$

205 Where Q_{MIP} and Q_{NIP} are tested adsorption capacities for MIP and NIP towards a template protein.

206 All of the measurements were carried out in triplicate, and the average values were chosen.

207

208 **Results and discussion**

209 **Synthesis of Silica Submicroparticles and Polymers**

210 Highly schematic representation of the preparation process for Lyz imprinted silica-based
211 polymers was shown in Fig. 1, which involved the following several steps: first, preparation of silica
212 submicroparticles; second, template protein prepolymerized with APTES on silica submicroparticles;
213 third, polymerization after addition of TEOS and HAc; finally removal of template. APTES was
214 chosen as the functional monomer, HAc (1.0 mol L⁻¹) and TEOS were used as a catalyst and cross
215 linking agent, respectively. In this work, SDS-HAc (10%w/v: 10%v/v) is selected as eluent to
216 remove the Lyz from MIPs and the eluate was detected by UV-vis spectrophotometer at the
217 wavelength of 278 nm for the quantitative analysis of Lyz eluted. The result validated that 51.03% of
218 Lyz was successfully washed away from MIPs. The result confirms the efficient removal of the
219 template for the MIPs. After the template molecules were removed, a great number of tailor-made
220 cavities for Lyz were left on the surface of silica submicroparticles. The uniform and small sizes of
221 the production obtained would offer high surface area for further recognition of template protein.

222 To further determine the structure of the silica-based MIP, FT-IR spectra of SiO₂ particles (a),
223 NIP (b) and MIP(c), were compared in Fig. 2. The wide and strong adsorption band around 3441

1
2
3
4 224 cm⁻¹ could be ascribed to stretching vibrations of O–H. The observed features near 470 cm⁻¹ and
5
6 225 1070 cm⁻¹ were the vibration peak and the anti-vibration peak of Si–O–Si, respectively. A
7
8
9 226 characteristic feature of MIP and NIP compared with silica submicroparticles were the special N–H
10
11 227 band around 1558 and 1417 cm⁻¹ from –NH₂ group and the C–H band around 2924 cm⁻¹ and 2852
12
13 228 cm⁻¹ from –CH₂ group. This FT-IR spectrum indicated that the APTES have been successfully
14
15
16 229 grafted onto the surface of silica submicroparticles after imprinting.
17

18
19 230 A series of polymers with varied degrees of cross-linking were prepared according to the Table
20
21 231 1. The adsorption capacities of the imprinted and non-imprinted polymers used different amounts of
22
23 232 TEOS as cross-linker were tested. The results indicated that the polymers MIP₂ employed 1.24 mL
24
25
26 233 of TEOS as cross-linker proved to have relatively better adsorption capacities for Lyz. The
27
28
29 234 recognition sites may be wrapped in the internal and the protein may be not easy to be eluted by
30
31 235 washing with a high cross-linking degree. Besides, polymers with a relatively low cross-linking
32
33
34 236 degree may have a variable three-dimensional structure which is unfavorable for rebinding.
35
36 237 Therefore, the MIP₂ with best adsorption capacity were selected in the following experiments.
37
38
39 238

239 **Characterization of the Imprinted Polymers by TEM and TG**

240 In order to investigate the network structure, the images of SiO₂, MIP and NIP observed by
241
242 241 TEM were shown in Fig. 3. From the results of the TEM pictures, uniform regular spherical
243
244 242 particle structure ranging from 0.42 to 0.52 μm in size could be obviously observed in all of
245
246 243 particles, which verified the successful formation of desired material shape and morphology. It
247
248 244 could be clearly observed that the average diameters among the SiO₂, MIP and NIP had no
249
250 245 significant difference. This meant the modified polymer layer were very thin which could facilitate
251
252
253
254
255
256
257
258
259
260

246 mass transfer and recognition in both elution process and rebinding process.

247 On the basis of the different thermal stability between the silica submicroparticles and the
248 polymers, TGA analysis was used to further study the relative composition of the silica core and the
249 polymers shell. As shown in Fig.4, when the temperature was changed from room temperature to
250 1000°C, the weight loss of silica was slight and approximately 10.0%, while the decrease of solvent
251 or water in weight was 6.0% at 200 °C, and the other decrease in weight was 4.0% at 200 - 700°C
252 (Fig. 4a). For silica @MIP, the weight loss was 25.0% at 700°C, while the decrease of solvent or
253 water in weight was about 12.0% at 200°C which was two times compared with that of silica
254 possibly due to the existing of imprinted cavity absorbing more water, and the other decrease in
255 weight was about 13.0% for the decomposition of imprinted polymer coatings at 200 - 700°C (Fig.
256 4c). If the mass retention of silica at 700°C is used as the reference, there exists near 15.0 wt%
257 difference in the weight retentions at 700 °C between silica and silica @MIP. It indicated that the
258 method applied for MIP coating in this work was excellently effective. The grafting yield of MIP
259 coating to silica was 15.0 wt%. In addition, the weight loss trend of silica @NIP (Fig. 4b) was
260 similar to silica @MIP and gave a result of 21.5%. Such distinction was due to the existence of
261 floccules-like imprinting coating on the surface of silica submicroparticles during the imprinting
262 process.

263

264 **Determination of Equilibrium Swelling Ratio**

265 The swelling ratio values of the SiO₂ particles, silica-based MIPs and NIPs were investigate by
266 immersion in PB overnight until swollen equilibrium, which were determined based on the amount
267 of water uptake. It was found that the SR value for NIPs was 1.96, which was lower than that

1
2
3
4 268 obtained with MIPs, where the SR value was 2.71. It is reasonable that the SR value for SiO₂
5
6 269 particles is the least only 1.03. Such results could possibly be due to the formation of binding
7
8
9 270 cavities on the surface of the MIPs, which enhanced water penetration and higher water uptake.
10
11 271 Higher SR value for MIP could lead to lower mass transfer resistance, which is important for loading
12
13
14 272 and release of the template in binding and extracting process respectively.
15
16
17
18
19 273

274 **Adsorption Kinetics**

20
21 275 In the evaluation for adsorption kinetics, the adsorption capacities of the imprinted and
22
23
24 276 non-imprinted polymers were tested as a function of time. The experiments were performed 10 mg
25
26 277 of MIP or NIP in 5.0 mL of 0.8 mg/mL initial Lyz concentration on the shaker (200 r/min, 25°C) for
27
28
29 278 incubation. The kinetics curves were shown in Fig.5. From the Fig.5, we can see that the adsorption
30
31 279 capacities of the polymers for Lyz increased as time goes by. The absorbance of MIP for Lyz had a
32
33
34 280 rapid increase in 2 h, and then slowed down with the time extension, finally reached equilibrium
35
36
37 281 after 5 h. This might be explained that Lyz was easy to reach the surface imprinting sites on the
38
39 282 Lyz-imprinted polymers at the starting. With the saturation of the sites, Lyz began to diffuse onto the
40
41
42 283 surface of Lyz-imprinted polymers nonspecifically. Obviously, the imprinted polymers adsorbed
43
44 284 more template protein compared to the non-imprinted polymers under the same conditions. This
45
46
47 285 result also confirmed the fact that recognition sites with the specific shape and the orientation of
48
49 286 functional groups successfully formed in the imprinted polymers network during the imprinting
50
51
52 287 process. The relatively higher adsorption capacity of the MIP compared with NIP could be attributed
53
54 288 to the hydrogen bonding interactions between functional groups of MIP and template protein, such
55
56
57 289 as amide group, amino group, and hydroxyl group. In addition, MIP needed longer time than NIP to
58
59
60

1
2
3
4 290 get equilibrium because it contained the deep caves left by template molecules.
5
6

7 291

8 292 **Adsorption Isotherms**

9
10
11 293 To investigate the binding capacity for Lyz of both MIP and NIP, the adsorption isotherms were
12
13 294 tested in the range of 0.2–1.1 mg/mL initial concentration of Lyz. The adsorption experiments were
14
15 295 accomplished as the previous procedures. The effect of the initial Lyz concentrations on the adsorption
16
17 296 capacities of the imprinted and the non-imprinted polymers prepared by the same conditions were
18
19 297 investigated under room temperature and the results were showed in Fig. 6. As the figure showed, the
20
21 298 equilibrium adsorption capacities of the MIP and NIP rose with the increase of the initial Lyz
22
23 299 concentrations from 0.2 to 0.8 mg/mL. Then the curve became flat and reached thermodynamic
24
25 300 equilibrium in the concentration region of above 0.8 mg/mL. Taking into account that Lyz was
26
27 301 insoluble in water with high concentration, the concentration of 0.8 mg/mL was chosen as the optimal
28
29 302 condition for the following experiments. It also found that the MIP had comparatively higher Lyz
30
31 303 adsorption capacities than the NIP in all the tested Lyz solutions, and the imprinting factor α reached
32
33 304 2.53. In our study, the high adsorption capacity for Lysozyme may be explained by the formation of
34
35 305 specific imprinting sites with complementary size and shape in MIP to hold and fix the Lysozyme
36
37 306 molecular around MIP. The remaining silanol groups on the surface of the silica cores might play a
38
39 307 important role on enrichment of the templates Lysozyme from the prepolymerization solution before
40
41 308 polymerization and co-operation with the functional and cross-linking monomers to create the
42
43 309 imprinting sites while polymerization process. Additionally, the advantages of the micro-sized MIP
44
45 310 with big specific surface area and surface energy also attributed to enhance the adsorption capacity for
46
47 311 Lysozyme. However, as for NIPs, the non-specific adsorption has dominant effect for lacking of
48
49
50
51
52
53
54
55
56
57
58
59
60

1
2
3
4 312 recognition sites. Therefore, the binding amount of Lyz is much lower. In addition, the MIP could be
5
6 313 reused twice without weakening the binding capacity significantly.
7

8
9 314 The adsorption experiment data of these polymers could be further processed according to
10
11 315 Langmuir adsorption equation to estimate the binding parameters which was proposed by Irving
12
13 316 Langmuir^[32]. This equation was well known for its preferably use at saturation conditions and more
14
15
16 317 homogeneous adsorbents such as the molecularly imprinted materials^[33-34]. The equation was listed as
17
18
19 318 following:

20
21 319
$$C_e/Q = C_e/Q_{max} + 1/(KQ_{max}) \quad (4)$$

22
23

24 320 Where C_e is the adsorption equilibrium concentration for Lyz, Q is the theoretical maximum
25
26 321 adsorption capacity for polymers, Q_{max} is the saturated adsorption after adsorption equilibrium, and
27
28 322 K is the Langmuir adsorption equilibrium constant. A highly linearized plot of C_e/Q versus C_e was
29
30 323 made. The Langmuir equation fits well for Lyz adsorption on MIP within the concentration range
31
32 324 studied (correlation coefficient, $r^2 = 0.99882$). The corresponding K and Q_{max} was 17.41 mL/mg
33
34 325 and 90.33 mg/g which were obtained from the slope and intercept of Langmuir equation simulated
35
36 326 curve. The result evidenced a relatively high adsorption affinity of our synthesized MIP for Lyz.
37
38
39
40

41 327

42 43 328 **Selectivity of the Polymers**

44
45
46 329 In this experiment, BHB, BSA, OVA were selected as reference proteins with a test
47
48
49 330 concentration of 0.8 mg/mL to study the selectivity of MIP for Lyz. This choice was based on the
50
51 331 fact that reference proteins had a various shape, isoelectric point and molecular weight compared to
52
53 332 the template Lyz. The adsorption capacities results of the MIP and NIP for different proteins were
54
55
56 333 illustrated in Fig. 7. As shown in Fig. 7, MIP displayed a highest adsorption capacity for Lyz among
57
58
59
60

1
2
3
4 334 the four test protein substrates, indicating the high adsorption selectivity for Lyz. Moreover, a
5
6 335 comparison of the adsorption of the MIP and NIP for each protein substrate suggested that the MIP
7
8
9 336 hardly showed an imprinting effect for BHb, BSA, OVA as both MIP and NIP nearly had the same
10
11 337 adsorption capacity for them.

12
13
14 338 The selectivity factor β was used to evaluate the specific selectivity and defined by following
15
16 339 formula:

17
18
19 340
$$\beta = \alpha_{\text{Lyz}} / \alpha_{\text{RP}} \quad (5)$$

20
21 341 Where α_{Lyz} and α_{RP} were tested imprinting factor of polymer for template protein Lyz and particular
22
23 342 reference proteins. The values of imprinting factor α and selectivity factor β for Lyz, BHb, BSA and
24
25 343 OVA were easily obtained by simple calculations and presented in Table 2. It was observed that α
26
27 344 values of MIP for Lyz relative to BHb, OVA and BSA were much higher, which meant that the
28
29 345 imprinted polymer possessed pronounced adsorption selectivity for the template Lyz as compared with
30
31 346 other reference proteins. In addition, the β values for BHb, BSA and OVA were far more than 1.0,
32
33 347 which again indicated the MIP had higher adsorption selectivity than that of the NIP. The preferred
34
35 348 adsorption for the template Lyz might be owing to the existence of memory recognition sites
36
37 349 formed in MIP during imprinting process, which were perfectly complementary fit with the template
38
39 350 Lyz both in shape and size. So the different spatial orientation of reference proteins did not match the
40
41 351 imprinted cavities and its access to the binding sites might be limited by the steric hindrance of
42
43 352 polymer chains, thus the adsorption capacity is relatively low and mainly comes from physical
44
45 353 adsorption associated with nonspecific interactions.
46
47
48
49
50
51
52
53
54
55
56
57
58
59
60

1
2
3
4 356 **Conclusions**
5

6 357 In our research, a new kind of surface molecular imprinting polymer for template protein Lyz
7
8 358 used APTES as functional monomer and TEOS as cross-linker had been successfully synthesized
9
10
11 359 based on supporting matrices silica submicroparticles. The optimal binding conditions were
12
13 360 investigated and gave a result of adsorption equilibrium time 5 h and initial protein concentrations
14
15 361 0.8 mg/mL with maximum experimental adsorption capacities of 84.13 mg/g and 33.19 mg/g for
16
17 362 MIP and NIP respectively. Batch binding experiments demonstrated product material offered fast
18
19 363 adsorption kinetic rate and MIP had significantly higher adsorption affinity for the template Lyz
20
21 364 compared with NIP in all cases. The equilibrium adsorption isotherms of Lyz on MIP could be well
22
23 365 fitted by the Langmuir adsorption model. At the same time, the MIP for Lyz exhibited good
24
25 366 selectivity over reference proteins with all separation factors larger than 2 by direct adsorption of the
26
27 367 single reference protein. The results of all the experiments suggested that specific recognition sites
28
29 368 which were sterically complementary to the template molecules Lyz were formed in the process of
30
31 369 the imprinting step, which was an essential favorable factor during the binding process. In addition,
32
33 370 the MIP could be reused twice without weakening the binding capacity significantly. All the
34
35 371 abovementioned properties such as easy preparation, fast mass transfer rate, satisfied adsorption
36
37 372 capacity, easy separation and specific recognition capability to the template protein Lyz made this
38
39 373 method and MIP material a promising prospect for the application in the field of rapid protein
40
41 374 separation and enrichment for the near future.
42
43
44
45
46
47
48
49
50

51 375
52
53
54
55
56
57 377
58
59
60

378 **Acknowledgements**

379 The authors greatly appreciate the financial supports by the National Natural Science
380 Foundation of China (No. 21175040; No. 21375035; No.J1210040) and the
381 Foundation for Innovative Research Groups of NSFC (Grant 21221003).

383 **References**

- 384 1 G. Vlatakis, L. I. Andersson, R. Müller and K. Mosbach, *Nature*, 1993, **361**, 645–647.
- 385 2 G. Wulff, *Chem. Rev.*, 2002, **102**, 1–27.
- 386 3 N. Masque', R. M. Marce', F. Borrull, P. A. G. Cormack and D. C. Sherrington, *Anal. Chem.*,
387 2000, **72**, 4122–4126.
- 388 4 B.-W. Wu, Z.-H. Wang, D.-X. Zhao and X.-Q. Lu, *Talanta*, 2012, **101**, 374–381.
- 389 5 Z.-H. Wang, H. Li, J. Chen, Z.-H. Xue, B.-W. Wu and X.-Q. Lu, *Talanta*, 2011, **85**, 1672–1679.
- 390 6 J. Li, T.-B. Liu, D.-L. Xiao, P. Dramou, W.-Y. Zou and H. He, *Chinese J. Anal. Chem.*, 2012, **40**,
391 1461–1468.
- 392 7 C. Baggiani, L. Anfossi and C. Giovannoli, *Anal. Chim. Acta*, 2007, **59**, 29–39.
- 393 8 F.-H. Lin, X.-J. Huang, D.-X. Yuan and S.-Y. Nong, *Chinese J. Anal. Chem.*, 2012, **40**, 243–248.
- 394 9 T.-H. Jiang, L.-X. Zhao, B.-L. Chu, Q.-Z. Feng, W. Yan and J.-M. Lin, *Talanta*, 2009, **78**,
395 442–447.
- 396 10 Y.-L. Hu, Y.-W. Li, R.-J. Liu, W. Tan and G.-K. Li, *Talanta*, 2011, **84**, 462–470.
- 397 11 M. Resmini, *Anal. Bioanal. Chem.*, 2012, **402**, 3021–3026.
- 398 12 X.-T. Shen, L.-H. Zhu, G.-X. Liu, H.-Q. Tang, S.-S. Liu and W.-Y. Li, *New J. Chem.*, 2009, **33**,
399 2278–2285.
- 400 13 J. Z. Hilt and M. E. Byrne, *Adv. Drug Delivery Rev.*, 2004, **56**, 1599–1620.
- 401 14 C. Alexander, H. S. Andersson, L. I. Andersson, R. J. Ansell, N. Kirsch, I. A. Nicholls, J.
402 O'Mahony and M. J. Whitcombe, *J. Mol. Recognit.*, 2006, **19**, 106–180.
- 403 15 S. M. Reddy, Q. T. Phan and H. El-Sharif, *Biomacromolecules*, 2012, **13**, 3959–3965.
- 404 16 M. E. Brown and D. A. Puleo, *Chem. Eng. J.*, 2008, **137**, 97–101.
- 405 17 J. Gao, H. Tian and Y. Wang, *Biomaterials*, 2012, **33**, 3344–3352.
- 406 18 Y. Jin, M. Jiang, Y. Shi, Y. Lin, K. Peng and B. Dai, *Anal. Chim. Acta*, 2008, **612**, 105–113.

- 1
2
3 407 19 Q.-Z. Feng, L.-X. Zhao, W. Yan, J.-M. Lin and Z.-X. Zheng, *J. Hazard. Mater.*, 2009, **167**,
4 408 282–288.
5
6
7 409 20 C.-Y. Huang, M.-J. Syu, Y.-S. Chang, C.-H. Chang, T.-C. Chou and B.-D. Liu, *Biosens.*
8
9 410 *Bioelectron.*, 2007, **22**, 1694–1699.
10
11 411 21 J. L. Urraca, M. C. Moreno-Bondi, G. Orellana, B. Sellergren and A. Hall, *J. Anal. Chem.*, 2007,
12 412 **79**, 4915–4923.
13
14 413 22 B.-J. Gao, J. Wang, F.-Q. An and Q. Liu, *Polymer*, 2008, **49**, 1230–1238.
15
16 414 23 X.-T. Shen, L.-H. Zhu, G.-X. Liu, H.-W. Yu and H.-Q. Tang, *Environ. Sci. Technol.*, 2008, **42**,
17 415 1687–1692.
18
19 416 24 Y.-L. Hu, R.-J. Liu, Y. Zhang and G.-K. Li, *Talanta*, 2009, **79**, 576–582.
20
21 417 25 Y. Li, X. Li, C.-K. Dong, J.-Y. Qi and X.-J. Han, *Carbon*, 2010, **48**, 3427–3433.
22
23 418 26 D.-M. Gao, Z.-P. Zhang, M.-H. Wu, C.-G. Xie, G.-J. Guan and D.-P. Wang, *J. Am. Chem. Soc.*,
24 419 2007, **129**, 7859–7866.
25
26 420 27 H.-Y. He, G.-Q. Fu, Y. Wang, Z.-H. Chai, Y.-Z. Jing and Z.-L. Chen, *Biosens. Bioelectron.*,
27 421 2010, **76**, 760–765.
28
29 422 28 M.-J. Meng, Z.-P. Wang, L.-L. Ma, M. zhang, J. Wang, X.-H. Dai and Y.-S. Yan, *Ind. Eng.*
30 423 *Chem. Res.*, 2012, **51**, 14915-14924.
31
32 424 29 J. E. Lofgreen and G. A. Ozin, *Chem. Soc. Rev.*, 2014, **43**, 911-933.
33
34 425 30 T. Shiomi, M. Matsui, F. Mizukami and K. Sakaguchi, *Biomaterials*, 2005, **26**, 5564–5571.
35
36 426 31 W. Stöber, A. Finker and E. J. Bohn, *J. Colloid Interface Sci.*, 1968, **26**, 62–69.
37
38 427 32 I. Langmuir, *J. Am. Chem. Soc.*, 1916, **38**, 2221-2295.
39
40 428 33 J. Aburto, A. Mendez-Orozco and S. L. Borgne, *Chem. Eng. Process*, 2004, **43**, 1587-1595.
41
42 429 34 R. J. Umpleby, S. C. Baxter, Y. Chen, R. N. Shah and K. D. Shimizu, *Anal. Chem.*, 2001, **73**,
43 430 4584-4591.
44
45 431
46 432
47 433
48 434
49 435
50 436
51 437
52 438
53 439
54 440
55 441
56
57
58
59
60

1
2
3 442 **Table captions**

4 443 Table 1 Preparation different degrees of cross-link polymers

5 444 Table 2 Values of imprinting factor α and selectivity factor β for Lyz, BHb, BSA and OVA

6 445

7 446

8 447

9 448

10 449

11 450

12 451

13 452

14 453

15 454

16 455

17 456

18 457

19 458

20 459

21 460

22 461

23 462

24 463

25 464

26 465

27 466

28 467

29 468

30 469

31 470

32 471

33 472

34 473

35 474

36 475

37 476

38 477

39 478

40 479

41 480

42 481

43 482

44 483

45 484

46 485

47

48

49

50

51

52

Polymers	SiO ₂ (g)	Lyz (g)	APTES(mL)	TEOS(mL)	HAc (mL)	Ethanol (mL)	PB(mL)
MIP ₁	0.400	0.100	0.620	0.620	1.000	20	20
MIP ₂	0.400	0.100	0.620	1.240	1.000	20	20
MIP ₃	0.400	0.100	0.620	1.860	1.000	20	20
NIP ₁	0.400		0.620	0.620	1.000	20	20
NIP ₂	0.400		0.620	1.240	1.000	20	20
NIP ₃	0.400		0.620	1.860	1.000	20	20

486 **Table 1 preparation different degrees of cross-link Polymers**

487

488

489

490

491

492

493

494

495

496

497

498

499

500

501

502

503

504

505

506

507

508

509

510

511

512

513

514

Protein	Lyz	BHb	BSA	OVA
Imprinting factor α	2.53	1.14	1.07	1.13
Selectivity factor β		2.22	2.36	2.24

Table 2 Values of imprinting factor α and selectivity factor β for Lyz, BHb, BSA and OVA

1
2
3
4
5
6
7
8
9
10
11 515
12 516
13 517
14 518
15 519
16 520
17 521
18 522
19 523
20 524
21 525
22 526
23 527
24 528
25 529
26 530
27 531
28 532
29 533
30 534
31 535
32 536
33 537
34 538
35 539
36 540
37 541
38 542
39 543
40 544
41 545
42 546
43 547
44 548
45 549
46 550
47 551
48 552
49
50
51
52
53
54
55
56
57
58
59
60

1
2
3
4
5
6
7
8
9
10
11
12
13
14
15
16
17
18
19
20
21
22
23
24
25
26
27
28
29
30
31
32
33
34
35
36
37
38
39
40
41
42
43
44
45
46
47
48
49
50
51
52
53
54
55
56
57
58
59
60553 **Figure captions**

554 Figure 1.Schematic representation of the molecular imprinting procedures.

555 Figure 2.FT-IR spectra of SiO₂ (a), NIP (b) and MIP(c).556 Figure 3.TEM images of SiO₂ (a), MIP (b) and NIP(c).557 Figure 4.TGA Curves of SiO₂ (a), NIP (b) and MIP(c).

558 Figure 5.Binding kinetics curve of the Lyz on MIP and NIP.

559 Figure 6.Adsorption isotherms of the Lyz on MIP and NIP.

560 Figure 7.Selective adsorption between reference proteins and Lyz on MIP and NIP.

561

562

563

564

565

566

567

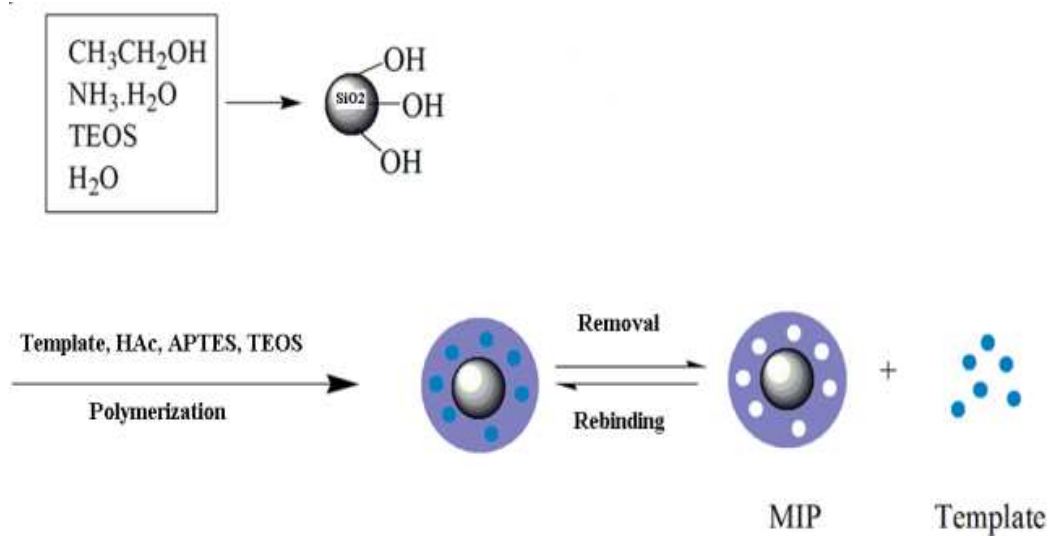
568

569

570

571

572



573

574 Figure 1. Schematic representation of the molecular imprinting procedures.

575

576

577

578

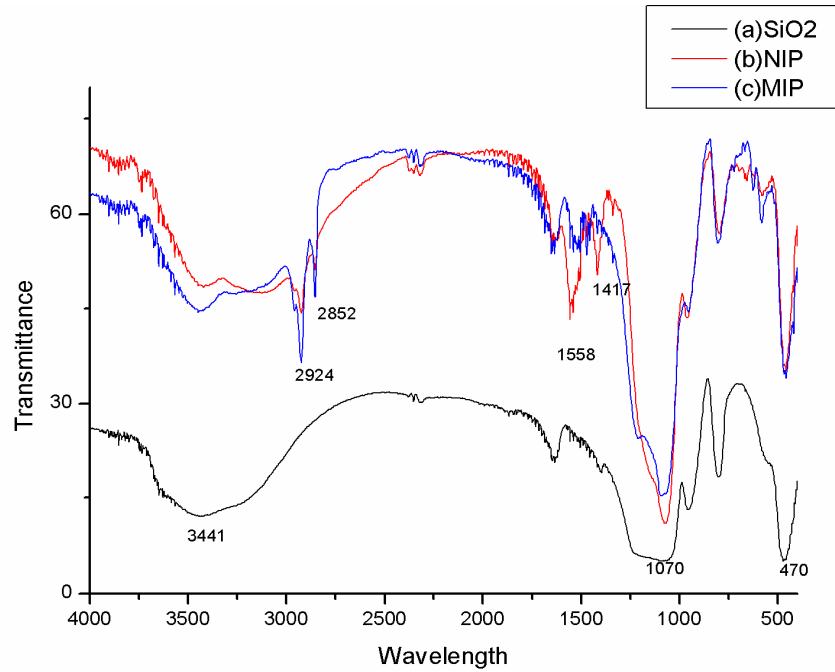
579

580

581

582

583



584

585 Figure 2. FT-IR spectra of SiO₂ (a), NIP (b) and MIP (c).

586

587

588

589

590

591

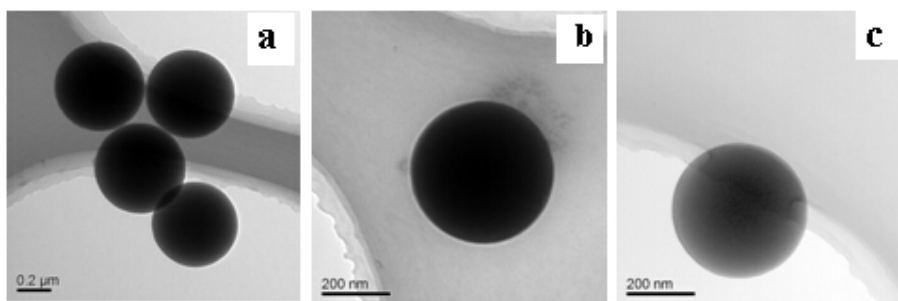
592

593

594

595

596



597

598 Figure 3. TEM images of SiO₂ (a), MIP (b) and NIP(c).

599

600

601

602

603

604

605

606

607

608

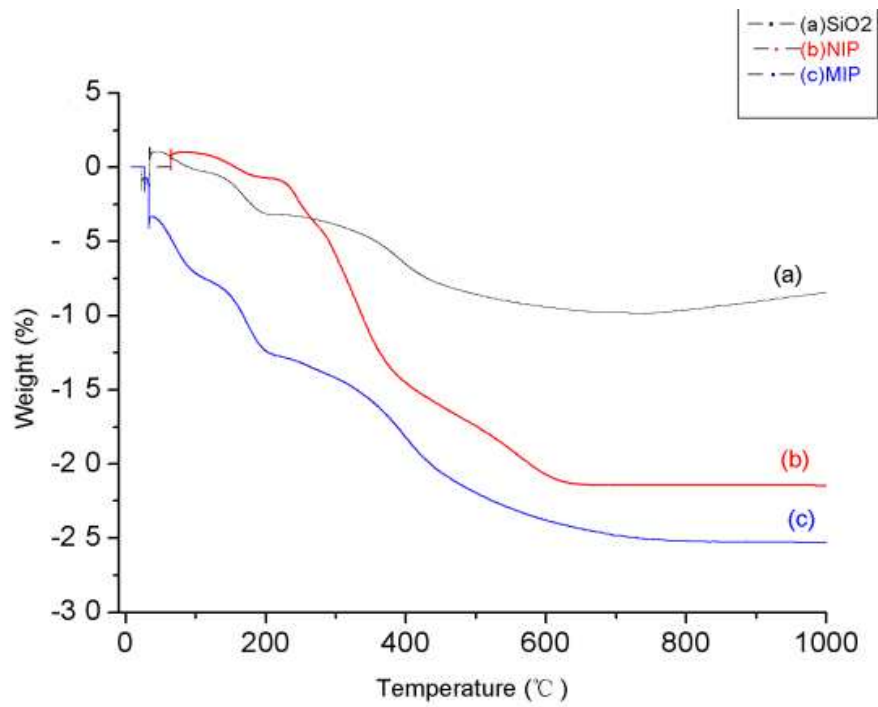
609

610

611

612

613



614

615 Figure 4.TGA Curves of SiO₂ (a), NIP (b) and MIP(c).

616

617

618

619

620

621

622

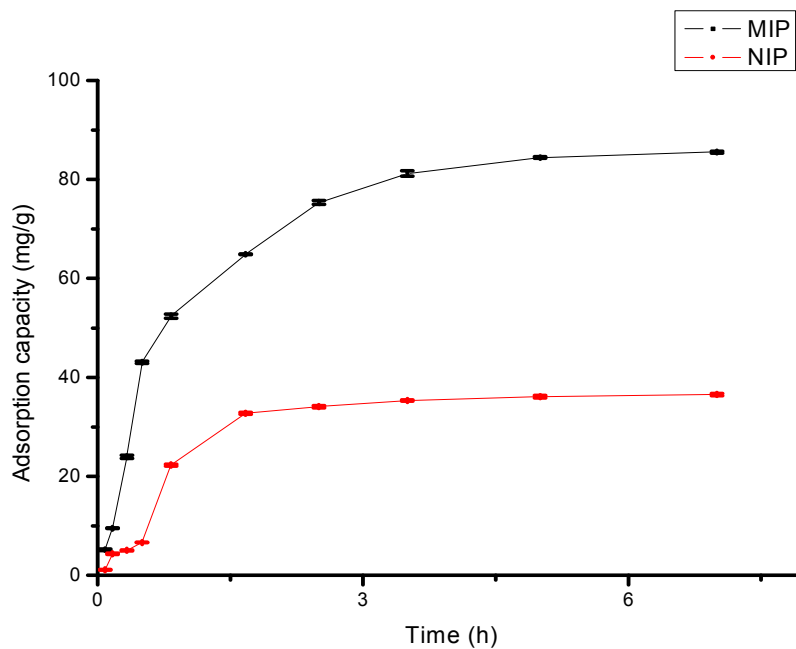
623

624

625

626

627



628

629 Figure 5. Binding kinetics curve of the Lyz on MIP and NIP (mean \pm s; n=3).

630

631

632

633

634

635

636

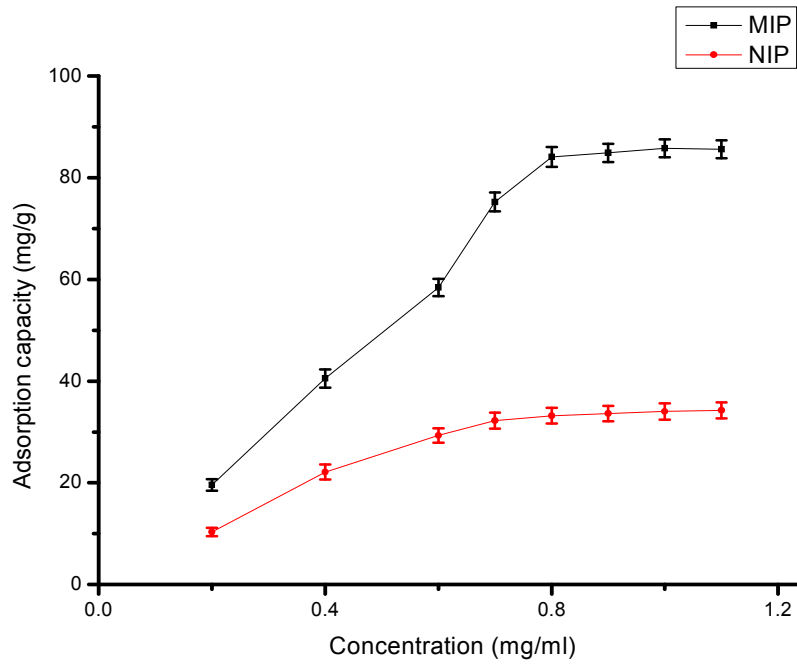
637

638

639

640

641



642

643 Figure 6. Adsorption isotherms of the Lyz on MIP and NIP (mean \pm s; n=3).

644

645

646

647

648

649

650

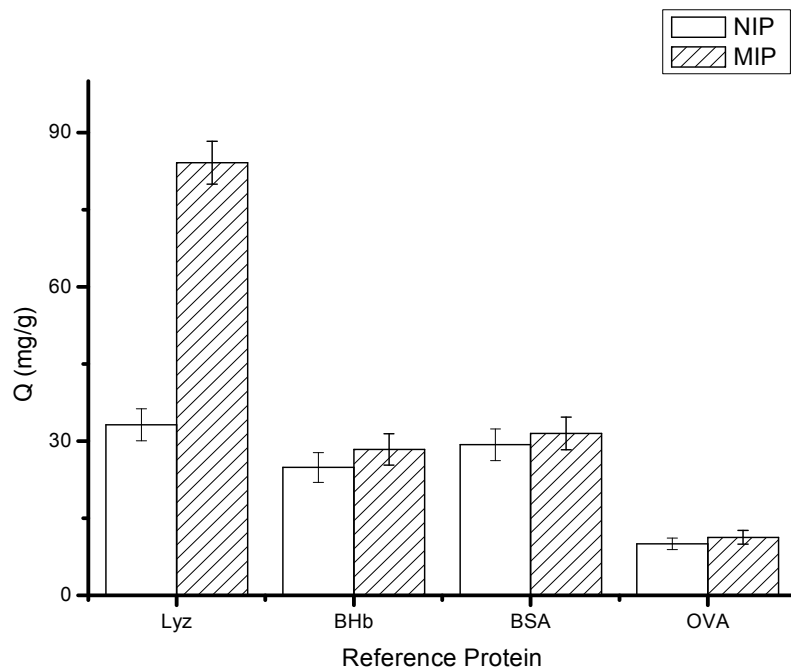
651

652

653

654

655



656

657 Figure 7. Selective adsorption between reference proteins and Lyz on MIP and NIP (mean \pm s;

658 n=3).